

L. Ya. Aranovich · R. C. Newton

H₂O activity in concentrated KCl and KCl-NaCl solutions at high temperatures and pressures measured by the brucite-periclase equilibrium

Received: 9 August 1996 / Accepted: 15 November 1996

Abstract H₂O activities in supercritical fluids in the system KCl-H₂O-(MgO) were measured at pressures of 1, 2, 4, 7, 10 and 15 kbar by numerous reversals of vapor compositions in equilibrium with brucite and periclase. Measurements spanned the range 550–900 °C. A change of state of solute KCl occurs as pressures increase above 2 kbar, by which H₂O activity becomes very low and, at pressures of 4 kbar and above, nearly coincident with the square of the mole fraction ($x_{\text{H}_2\text{O}}$). The effect undoubtedly results primarily from ionic dissociation as H₂O density ($\rho_{\text{H}_2\text{O}}$) approaches 1 gm/cm³, and is more pronounced than in the NaCl-H₂O system at the same *P-T-X* conditions. Six values of solute KCl activity were yielded by terminal points of the isobaric brucite-periclase *T*- $x_{\text{H}_2\text{O}}$ curves where sylvite saturation occurs. The H₂O mole fraction of the isobaric invariant assemblage brucite-periclase-sylvite-fluid is near 0.52 at all pressures, and the corresponding temperatures span only 100 °C between 1 and 15 kbar. This remarkable convergence of the isobaric equilibrium curves reflects the great influence of pressure on lowering of both KCl and H₂O activities. The H₂O and KCl activities can be expressed by the formulas: $a_{\text{H}_2\text{O}} = \gamma_{\text{H}_2\text{O}}[x_{\text{H}_2\text{O}}/(x_{\text{H}_2\text{O}} + (1 + \alpha)x_{\text{KCl}})]$, and $a_{\text{KCl}} = \gamma_{\text{KCl}}[(1 + \alpha)x_{\text{KCl}}/(x_{\text{H}_2\text{O}} + (1 + \alpha)x_{\text{KCl}})]^{(1+\alpha)}$, where α is a degree of dissociation parameter which increases from zero at the lowest pressures to near one at high pressures and the γ 's are activity coefficients based on an empirical regular solution parameter *W*: $\ln \gamma_i = (1 - x_i)^2 W$. Least squares fitting of our H₂O and KCl activity data evaluates the parameters: $\alpha = \exp(4.166 - 2.709/\rho_{\text{H}_2\text{O}} - 212.1P/T)$, and $W = (-589.6 - 23.10P)/T$, with $\rho_{\text{H}_2\text{O}}$ in gm/cm³, *P* in kbar and *T* in K. The standard deviation from the measured activities is only ± 0.014 . The equations define isobaric liquidus curves, which are in perfect agreement with previous DTA liq-

uidus measurements at 0.5–2 kbar, but which depart progressively from their extrapolation to higher pressures because of the pressure-induced dissociation effect. The great similarity of the NaCl-H₂O and KCl-H₂O systems suggests that H₂O activities in the ternary NaCl-KCl-H₂O system can be described with reasonable accuracy by assuming proportionality between the binary systems. This assumption was verified by a few reconnaissance measurements at 10 kbar of the brucite-periclase equilibrium with a Na/(Na + K) ratio of 0.5 and of the saturation temperature for Na/(Na + K) of 0.35 and 0.50. At that pressure the brucite-periclase curves reach a lowest $x_{\text{H}_2\text{O}}$ of 0.45 and a temperature of 587 °C before salt saturation occurs, values considerably lower than in either binary. This double-salt eutectic effect may have a significant application to natural polyionic hypersaline solutions in the deep crust and upper mantle in that higher solute concentrations and very low H₂O activities may be realized in complex solutions before salt saturation occurs. Concentrated salt solutions seem, from this standpoint, and also because of high mechanical mobility and alkali-exchanging potential, feasible as metasomatic fluids for a variety of deep-crust and upper mantle processes.

Introduction and previous work

Potassium species are important constituents of metamorphic fluids. Potassium metasomatism has been recognized by field workers in high-grade metamorphic terranes for over a century (e.g. Billings 1938). Alkali exchange in natural feldspars (K-feldspathization) gives rise to “replacement antiperthite”, a texture described many times in high-grade gneisses (Griffin 1969; Todd and Evans 1994; Hansen et al. 1995). The apparent ease of alkali exchange and migration in metamorphic rocks has led to classification of alkalis with the volatiles as “perfectly mobile components” (Korzhinskii 1959). This high alkali mobility may be understandable in terms of transport in intergranular brines (Aranovich et al.

L. Ya. Aranovich (✉) · R.C. Newton
Dept. of the Geophysical Sciences,
The University of Chicago,
Chicago, IL 60637, USA

Editorial responsibility: T. Grove

1987). Orville (1963) and Iiyama (1965) showed experimentally that feldspars exchange alkali ions easily with relatively dilute chloride and carbonate solutions at 1–2 kbar and 600–800 °C. For chloride solutions coexisting with both albite and K-feldspar, the $K/(K+Na)$ ratio is about 0.2. The preference of feldspar for potassium relative to supercritical brines may be a major factor in K-metasomatism and the production of NaCl-rich fluids in the crust.

The influence of higher pressures and higher salinities on the thermodynamic behavior of aqueous KCl solutions is an important consideration for understanding metasomatic processes at deep-earth conditions. Most critical for petrogenetic interpretations are the activities of the alkali chlorides and H_2O in concentrated supercritical solutions. The solution interaction of KCl and NaCl and its possible variation with pressure and temperature must be known in order to make predictions about alkali transport and conditions under which partial melting may occur in rock systems.

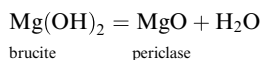
Sylvite (KCl) has been identified as a daughter mineral in some of the concentrated brine inclusions which have been described with increasing frequency in many petrogenetic settings, including granites (Dunbar et al. 1996), gabbros (Pasteris et al. 1995), high-grade gneisses (Touret 1985), carbonatites (Sampson et al. 1995), eclogites (Philippot and Selverstone 1991), and the super-high-pressure coesite-bearing metasediments (Philippot et al. 1995). KCl is thought to have been a major solute of the complex saline fluids which produced regional metasomatism and metal ore segregation in Cloncurry, Queensland (DeJong and Williams 1995) and the Melones Fault Zone of California (Albino 1995). Description of the thermodynamic properties of aqueous KCl solutions thus has potential application to a large variety of crustal processes.

Existing experimental work on the system KCl- H_2O is summarized by Sterner et al. (1992). The salt saturation surfaces in the binary system and in the ternary system with NaCl were constructed analytically based principally on the differential thermal analysis studies to 2 kbar of Chou et al. (1992). For compositions near the binary KCl-NaCl join, the ternary fluids may be represented adequately by a subregular solution involving five empirical Margules parameters which are functions of temperature and pressure.

Sylvite and halite (NaCl), though isostructural, have a broad asymmetric miscibility gap with a critical temperature near 500 °C, which rises substantially with pressure. The most comprehensive experimental work on the solvus is that of Bhardwaj and Roy (1971), with accurate delineation between 1 bar and 20 kbar. The equations of Sterner et al. (1992) incorporate this experimental work. The solvus intersects the NaCl-KCl- H_2O solidus in a complex way depending on temperature (T), pressure (P), and H_2O mole fraction (x_{H_2O}) of the liquids, resulting in cotectic melting over a substantial portion of P - T - X space. Elsewhere in the supercritical region at elevated pressures melting is of the smooth

minimum type, with the minimum composition near $K/(K + Na) = 0.5$ at pressures up to 2 kbar.

Aranovich and Newton (1996) encountered large, previously unpredicted changes in the thermodynamic mixing properties of NaCl- H_2O fluids with increasing pressure above 2 kbar. They measured H_2O activities in concentrated NaCl- H_2O solutions in the pressure range 2–15 kbar and temperature ranges 600–900 °C and NaCl concentrations up to halite saturation by depression of the equilibrium temperature of the reaction:



Compositions of the H_2O -NaCl fluid phase in equilibrium with brucite plus periclase at fixed T and P were determined by reversed experiments. Additional precise equilibrium data on this reaction with pure H_2O were obtained at 2–15 kbar to provide a reliable baseline for activity calculations. Termination of the isobaric brucite-periclase dehydration curves in the system MgO- H_2O -NaCl by halite saturation provided five independent values for NaCl activity in concentrated solutions in the supercritical region. The H_2O and NaCl activity data could be described within the experimental reversal brackets by the expressions:

$$a_{H_2O} = \frac{x_{H_2O}}{x_{H_2O} + (1 + \alpha)x_{NaCl}} \quad (1a)$$

$$a_{NaCl} = \left[\frac{(1 + \alpha)x_{NaCl}}{x_{H_2O} + (1 + \alpha)x_{NaCl}} \right]^{(1+\alpha)} \quad (1b)$$

These expressions imply that H_2O and NaCl are ideal mixtures of H_2O molecules and NaCl of variable degree of dissociation α which depends on temperature and pressure but not on composition. The parameter α was defined by least-squares fitting of the experimental data:

$$\alpha = \exp(A - B/\rho) - CP/T \quad (2)$$

where ρ is the density of pure H_2O at (T, P), and A , B , and C are positive constants.

The above formulation embodies a novel experimental finding, namely that activity in NaCl solutions decreases exponentially with pressure above 2–4 kbar at constant composition and temperature. At pressures approaching 10 kbar, H_2O activity becomes nearly equal to the square of its mole fraction. This effect most probably derives from pressure-induced dissociation of NaCl to Na^+ and Cl^- : α approaches one as H_2O densities approach 1 gm/cm³. Because of the physicochemical similarity among the alkali chlorides, analogous pressure-induced changes in solute behavior may be expected for KCl also.

An important implication of the low H_2O activities in concentrated brines at high pressures is that these fluids may coexist with silicate rocks at deep crust and upper mantle conditions without provoking extensive melting, while providing an effective vehicle for metasomatism and material transport, especially of the alkalis. The H_2O activities may be low enough in very concentrated

solutions to be possible fluid media in granulite facies metamorphism, where anhydrous mafic silicates (garnet and pyroxenes) dominate over hydrous phases (biotite and amphibole). The properties of alkali mobility and ease of infiltration in silicate rocks at low porosity are much superior to those of $\text{CO}_2\text{-H}_2\text{O}$ mixtures of comparably low H_2O activity, fluids which have long been assumed to be important in granulite facies metamorphism, but which are now known to have extremely low solubilities for silicate constituents and low wetting ability in dense silicate aggregates (Watson and Brenan 1987, Walther 1992). The present work explores H_2O and solute activities in the system $\text{KCl-H}_2\text{O}$ at deep crust/upper mantle $P\text{-}T$ conditions, with reconnaissance measurements in the ternary $\text{KCl-NaCl-H}_2\text{O}$ system, in order to describe more completely the thermodynamic behavior of supercritical alkali chloride brines in the geological context.

Experimental methods

Experimental methods were mainly those employed by Aranovich and Newton (1996). Charges consisting of weighed portions of synthetic brucite, periclase, KCl , NaCl and H_2O were sealed in 1 mm diameter Pt tube segments. The periclase was a coarsely crystalline material prepared by arc-fusion. Use of this starting material eliminated the quench-reaction problem encountered by previous workers who used extremely fine-grained periclase. The experiments at 4, 7, 10 and 15 kbar were done in 1.91 cm diameter piston-cylinder apparatus with NaCl pressure medium and calibrated pairs of W-3% Rh vs W-25% Rh thermocouples, and in internally heated argon pressure vessels with sheathed Cr-Al thermocouples at one and two kbar. The pressure and temperature uncertainties in the piston-cylinder apparatus are ± 0.2 kbar and ± 3 °C, and are $\pm .01$ kbar and ± 2 °C in the gas pressure vessels. Two capsules with different charges were present in most runs in both kinds of apparatus.

Composition of the vapor phase at the conclusion of an experiment was determined by puncturing the charges under liquid N_2 (to avoid spurting of water) and drying at 320 °C for up to half an hour. A H_2O yield less than the amount originally introduced signified growth of brucite, the hydrate, whereas a H_2O yield greater than originally present signified H_2O release in decomposition of brucite to periclase. After a small amount of reconnaissance, it was generally possible to bracket an equilibrium composition in a single experiment: the two charges usually reacted in opposite directions with close approach of the fluid compositions to a common value. Confirmation of the direction of reaction was made optically and by X-ray diffraction.

Six determinations of points on the $\text{KCl-H}_2\text{O}$ saturation surface were yielded by termination of the isobaric brucite-periclase equilibrium curves. When the vapor is salt-saturated, the brucite-periclase curve will descend no further in temperature with increase of KCl in the bulk composition, but becomes invariant. The invariant temperature for coexisting brucite, periclase, sylvite and fluid at each of the six experimental pressures was determined by reversed reactions in charges containing small proportions of H_2O , guaranteeing sylvite saturation of the fluid.

Several experiments were made in the system $\text{KCl-NaCl-H}_2\text{O}$ (-MgO) to sketch out the ternary chloride brine system. According to the calculated melting diagram of Sterner et al. (1992), the binary system KCl-NaCl has a continuous isobaric melting loop with a broad minimum quite near to a KCl mole fraction of 0.5, and, with increasing H_2O content of the salt melts, the minimum shifts to higher KCl mole fraction and lower temperatures and intersects the solvus near $x_{\text{H}_2\text{O}} = 0.4$. A point on the $\text{KCl-NaCl-H}_2\text{O}$ minimum

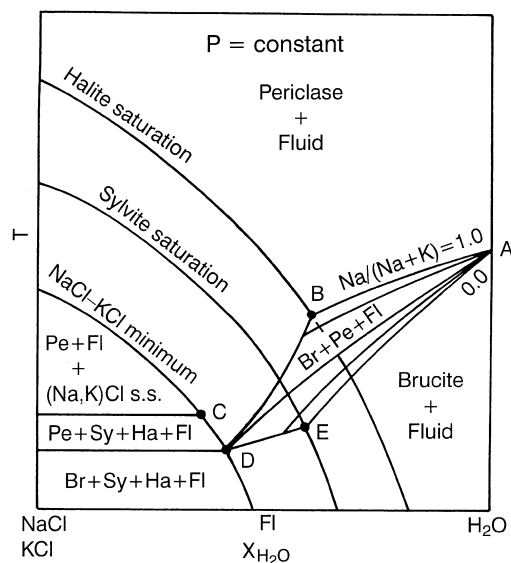


Fig. 1 Schematic univariant equilibria in the system $\text{KCl-NaCl-H}_2\text{O-MgO}$ at constant pressure in the supercritical fluid region. *Point A* is the brucite dehydration temperature for pure H_2O . *Curves between AB and AE* are brucite-periclase-fluid equilibria as functions of chloride concentration for fixed NaCl/KCl ratios. *Curves BD and ED* are, respectively, the univariant intersections of the brucite-periclase-fluid surface with the saturation surface of halite solid solution and the saturation surface of sylvite solid solution. *Point D* is an invariant 5-phase point on the salt saturation minimum curve. At temperatures higher than *Point C*, the minimum has a continuous tangent, whereas below *C* the minimum is of the cotectic type. A unique brucite-periclase-fluid curve *AD* of fixed NaCl/KCl terminates at the invariant point of four solids plus fluid; all other curves between *AB* and *AE* terminate on one or the other salt saturation surface. The diagram assumes that the fluid phase is strictly ternary (with negligible Mg content). *Sy* sylvite, *Ha* halite, *Fl* fluid, *s.s.* solid solution

melting curve at 10 kbar was determined using the brucite-periclase equilibrium. At fixed pressure, there exists a univariant locus of lowest melting temperature as a function of H_2O mole fraction. A unique brucite-periclase curve for fixed $\text{Na}/(\text{Na} + \text{K})$ in the fluid terminates on the salt saturation minimum curve (Fig. 1). Geometrical constraints indicated that the parameters of this intersection at 10 kbar are close to $x_{\text{H}_2\text{O}} = 0.45$, $\text{Na}/(\text{Na} + \text{K}) = 0.4$ and $T = 590$ °C. Several reversal runs with initial parameters embracing the above values were made to define invariant parameters of the equilibrium brucite-periclase-halite solid solution – sylvite solid solution – fluid. The method of these runs was identical in principle to the sylvite saturation experiments.

Quenched solid salt in the KCl-NaCl experiments was always two-phase, with compositions close to the end-members, whether the salt phase during the experiments was fluid or a homogeneous solid solution. Apparently, reequilibration is so rapid that high-temperature solid solutions cannot be quenched with our apparatus. This fact presented no difficulties of interpretation, inasmuch as the solvus is very well known to 20 kbar from the experimental work of Bhardwaj and Roy (1971).

Results of experiments and interpretation

Table 1 gives details of the experiments defining isobaric univariant brucite-periclase curves in the $\text{KCl-H}_2\text{O-MgO}$ system and the six experimental data for the isobaric sylvite saturation curves. The data are plotted in Fig. 2. The isobaric brucite-periclase curves are well-

Table 1 Experimental data on the reaction Brucite (*Br*) = Periclase (*Per*) + H₂O in the presence of H₂O-KCl solutions (*n/r* small change in water content in the course of the run; *sat.*, runs under KCl-saturated conditions; *st.* initial; *fin.* final)

Run #	T °C	P kbar	Duration h	x _{H₂O} st.	x _{H₂O} fin.	Stable phase
K-54	850	15	50	0.86	0.883	Per
K-55	850	15	50	0.93	0.89	Br
K-73	830	15	53	0.81	0.858	Per
K-74	830	15	53	0.9	0.871	Br
K-45	800	15	48	0.76	0.793	Per
K-46	800	15	46	0.82	0.8	Br
K-47	750	15	66	0.66	0.7	Per
K-48	750	15	66	0.74	0.711	Br
K-65	720	15	122	0.68	0.656	Br
K-66	720	15	122	0.6	0.652	Per
K-50	700	15	120	0.56	0.603	Per
K-51	700	15	120	0.64	0.612	Br
K-76	650	15	89	0.3	0.39	Per, sat.
K-80	645	15	73	0.3	0.214	Br, sat.
K-28	800	10	74	0.94	0.93	Br
K-29	800	10	74	0.88	0.91	Per
K-32	780	10	47	0.82	0.864	Per
K-33	780	10	47	0.91	0.887	Br
K-20	750	10	45	0.77	0.799	Per
K-21	750	10	45	0.83	0.813	Br
K-5	750	10	27	0.74	0.799	Per
K-36	730	10	72	0.72	0.76	Per
K-37	730	10	72	0.8	0.776	Br
K-1	700	10	47	0.6	0.693	Per
K-4	700	10	55	0.76	0.712	Br
K-7	670	10	49	0.6	0.625	Per
K-8	670	10	49	0.7	0.631	Br
K-38	650	10	70	0.56	0.593	Per
K-39	650	10	70	0.64	0.608	Br
K-31	630	10	70	0.51	0.544	Per
K-30	630	10	70	0.59	0.556	Br
K-35	620	10	118	0.3	0.227	Br, sat.
K-40	625	10	72	0.3	0.437	Per, sat.
K-56	740	7	94	0.84	0.859	Per
K-57	740	7	94	0.92	0.875	Br
K-43	700	7	145	0.72	0.783	Per
K-44	700	7	145	0.81	0.784	Br
K-60	680	7	147	0.71	0.735	Per
K-61	680	7	147	0.76	0.737	Br
K-58	650	7	146	0.64	0.673	Per
K-59	650	7	146	0.71	0.669	Br
K-63	620	7	165	0.54	0.579	Per
K-64	620	7	165	0.6	0.572	Br
K-71	605	7	99	0.29	0.423	Per, sat.
K-62	600	7	165	0.29	0.235	Br, sat.
K-83	660	4	70	0.76	0.804	Per
K-84	660	4	70	0.86	0.812	Br
K-89	630	4	144	0.67	0.724	Per
K-90	630	4	144	0.74	0.722	Br
K-87	600	4	146	0.6	0.657	Per
K-88	600	4	146	0.67	0.644	Br
K-95	575	4	145	0.3	0.39	Per, sat.
K-93	570	4	138	0.3	0.272	Br, sat.
K-11	640	2	139	0.79	0.844	Per
K-12	640	2	139	0.91	0.873	Br
K-18	620	2	118	0.73	0.773	Per
K-19	620	2	118	0.78	0.763	Br
K-15	600	2	145	0.59	0.681	Per
K-16	600	2	145	0.7	0.694	Br, n/r
K-22	570	2	198	0.56	0.57	Per, n/r
K-23	570	2	198	0.62	0.572	Br
K-41	555	2	283	0.27	0.388	Per, sat.
K-70	550	2	190	0.29	0.261	Br, sat.
K-92	570	1	228	0.65	0.69	Per
K-91	570	1	228	0.75	0.711	Br
K-97	550	1	165	0.29	0.37	Per, sat.
K-96	540	1	168	0.3	0.36	Br, sat.

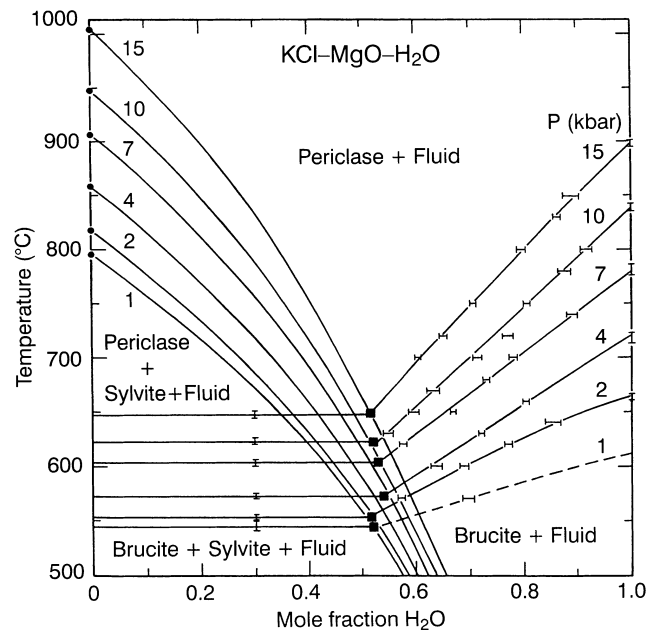


Fig. 2 Brucite-periclase-fluid equilibrium curves in the system KCl-MgO-H₂O at six pressures in the range 1–15 kbar determined by the reversed fluid-phase measurements. Data are given in Table 1. *Horizontal brackets* indicate approach to closure of final vapor compositions. *Vertical brackets* at $x_{\text{H}_2\text{O}} = 1.0$ are reversal intervals of the brucite-periclase equilibrium with pure H₂O fluid from Aranovich and Newton (1996). The *one-kbar curve* is only approximately constrained by one experimental bracket. Six isobaric sylvite saturation temperatures are determined by reversals of the H₂O concentration of fluids in equilibrium with either brucite or periclase and sylvite over narrow temperature intervals, as indicated by the *brackets* at $x_{\text{H}_2\text{O}} = 0.3$. The isobaric temperature-invariant brucite-periclase-sylvite-fluid lines intersect with their respective brucite-periclase-fluid curves in six points on the sylvite-fluid P - T - $x_{\text{H}_2\text{O}}$ saturation surface, as shown by the *black squares*. Isobaric sylvite saturation curves (hydrous melting curves) calculated from thermodynamic analysis of our brucite-periclase and sylvite saturation data are shown; the good agreement with the measured saturation points is evident. The limiting H₂O mole fraction of KCl-H₂O fluids in equilibrium with brucite and periclase is near 0.52; it is not certain if there is a real variation with pressure. *Filled circles* sylvite melting points from Clark (1959)

constrained by the reversal data. Slight curvature is indicated in the lower pressure range, whereas the curves for 4 kbar and above are nearly straight lines. The brucite-periclase curves terminate in invariant sylvite saturation points determined by the reversed experiments with initial $x_{\text{H}_2\text{O}} = 0.3$ in Table 1. The limiting H₂O mole fractions of the brucite-periclase curves average 0.52; a systematic pressure variation is not clear-cut. The six isobaric sylvite saturation curves, constructed from thermodynamic analysis, described below, of our experimental data, agree closely with the six measured saturation points (Fig. 2).

The outstanding feature of Fig. 2 is that the depression of the brucite-periclase equilibrium temperature at 10 and 15 kbar is much greater at a given H₂O concentration than at 1 and 2 kbar. This fact militates a dramatic decrease of H₂O activity in concentrated KCl

solutions with pressures above 2 kbar. The brucite decomposition temperature at any $x_{\text{H}_2\text{O}}$ of the fluid phase is somewhat lower than in NaCl-H₂O. Both of these findings are in fundamental accord with the results of the electrical conductance measurements (Quist and Marshall 1969; Quist et al. 1970), which demonstrated that the major increase in the conductance (i.e. degree of dissociation) of 0.01m KCl solutions occurs in the pressure range 1–3 kbar and that the KCl solutions exhibit higher conductance at any given P - T than NaCl solutions of the same concentrations.

Brucite in several of the run products was analyzed for Cl, including both high-pressure and low-pressure runs. None of the analyses showed Cl concentration exceeding 0.1 Cl atoms per 50 Mg atoms. Therefore, substitution of Cl in brucite is negligible in terms of the H₂O activity calculations.

Experiments were made to determine an upper bound on MgO solubility in concentrated KCl solutions at elevated pressure-temperature conditions. Two capsules with the normal amounts of KCl and H₂O (about 4 mg and 2 mg, respectively) and only 0.1 mg of periclase were held at 700 °C and 10 kbar for 48 h before quenching. The fluid compositions straddled the brucite-periclase field boundary, as previously determined. A charge with $x_{\text{H}_2\text{O}} = 0.67$ yielded abundant coarse-grained periclase with geometrically etched surfaces and no brucite. Nearly the original amount of periclase was recovered. Had the entire amount of periclase been dissolved, the maximum contribution of MgO to the fluid phase would have been only 1.5 mol%. In fact, the actual amount was much less than this. A charge with $x_{\text{H}_2\text{O}} = 0.73$ yielded abundant large geometrical brucite flakes (Fig. 3). A few relics of periclase jacketed with brucite were present. The two experiments together demonstrate that the MgO content of the fluids in our experiments was much too small to have influenced the activity measurements.

H₂O activities were retrieved from the vapor composition data using the tabulated fugacities of Burnham et al. (1969) and the expression of Aranovich and Newton (1996) for the standard Gibbs free energy of the pure H₂O brucite-periclase reaction at one bar:

$$\Delta G^\circ \text{ (joules)} = 73418 - 134.95 T \quad (3)$$

Compressibilities and thermal expansions of the solid phases were taken from Holland and Powell (1990). H₂O activities ($a_{\text{H}_2\text{O}}$) are given in Table 2. Figure 4 shows the same profound change of state of the salt solutions with pressure as shown by concentrated NaCl solutions: at pressures greater than 2 kbar, for H₂O densities greater than about 0.8 gm/cm³, H₂O activities decrease rapidly with compression and become nearly equal to the squares of the H₂O mole fractions. The exponential density dependence of $a_{\text{H}_2\text{O}}$ is even more pronounced than in NaCl solutions: at 4 kbar the high pressure behavior is effectively realized. Some further lowering of $a_{\text{H}_2\text{O}}$ with pressure occurs at 10 kbar and possibly even slightly more at 15 kbar.

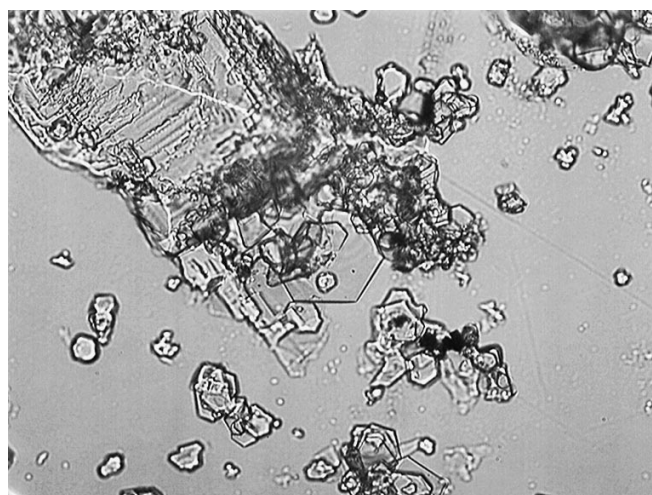


Fig. 3 Ordinary light photomicrograph of dried portion of quenched charge originally containing 3.94 mg KCl, 2.58 mg H₂O and 0.11 mg coarsely crystalline periclase. The experimental conditions were 700 °C, 10 kbar, and 48 h. The H₂O mole fraction of the fluid was 0.73, just within the brucite field (see Fig. 2). The experiment yielded abundant, large, geometrical brucite flakes, apparent in the photo (the largest grain seen is about 50 μm across), embedded in quench-precipitated sylvite. A companion run at the same conditions, with $x_{\text{H}_2\text{O}}$ of the fluid just outside the brucite field (0.67), yielded coarse periclase with etched surfaces and no brucite. These experiments demonstrate that MgO solubility in KCl-H₂O solutions at 10 kbar and 700 °C is much too small to have affected the activity measurements

KCl activities were calculated for the six sylvite saturation points terminating the brucite-periclase curves at each pressure. The standard molar entropy of melting, ΔS_m° , of KCl at the normal melting point of 1043 K is given by Robie et al. (1978) as 25.20 joules/K. The change of ΔS_m with temperature is quite small, according to Sterner et al. (1992), and the effect of pressure is uncertain. Therefore we have taken ΔS_m as a constant. KCl activities (a_{KCl}) were calculated from the expression:

$$\Delta S_m(T_{\text{sat}} - T_m) = RT_{\text{sat}} \ln a_{\text{KCl}} \quad (4)$$

where ΔS_m is the entropy of fusion of pure KCl, T_m is the melting point in K of pure sylvite at a given pressure and T_{sat} is the sylvite saturation temperature at that pressure and fixed H₂O mole fraction. The T_m values were taken from the melting-point equation of KCl given by Clark (1959). They agree exactly with the DTA measurements of Chou et al. (1992). The six a_{KCl} values yielded by the six isobaric saturation points are given in Table 2.

The exponential pressure decreases of $a_{\text{H}_2\text{O}}$ and a_{KCl} were modeled using formulas analogous to Eqs. (1a), (1b). However, the low H₂O activity values yielded by the brucite-periclase data necessitated an additional term multiplied to the expression for $a_{\text{H}_2\text{O}}$:

$$\gamma_{\text{H}_2\text{O}} = \exp[W_{\text{KH}} a_{\text{KCl}}^2] \quad (5a)$$

where $\gamma_{\text{H}_2\text{O}}$ is a binary activity coefficient and W_{KH} is a regular solution Margules parameter which depends on

Table 2 Measured H₂O activity from brucite-periclase reversals and KCl activity from sylvite saturation temperatures^a

<i>P</i> kbar	<i>T</i> °C	$\bar{x}_{\text{H}_2\text{O}}$	$f_{\text{H}_2\text{O}}$ bar	$\rho_{\text{H}_2\text{O}}$ gm/cm ³	$a_{\text{H}_2\text{O}}$	a_{KCl}	$\Gamma_{\text{H}_2\text{O}/\text{KCl}}$
15	850	.887	45747	.973	.815		.919
15	830	.865	45580	.980	.737		.852
15	800	.797	45407	.991	.628		.788
15	750	.706	45045	1.009	.472		.669
15	720	.654	44922	1.020	.391		.598
15	700	.608	44679	1.027	.344		.566
15	647*	.515		1.050		.308	.635
10	800	.920	16214	.885	.833		.915
10	780	.876	15829	.893	.751		.857
10	750	.805	15331	.905	.634		.788
10	730	.768	14921	.913	.565		.736
10	700	.703	14318	.925	.472		.671
10	670	.628	13646	.938	.391		.623
10	650	.601	13193	.946	.342		.569
10	630	.550	12711	.954	.298		.542
10	623*	.520		.957		.333	.694
7	740	.867	7174	.811	.784		.904
7	700	.783	6692	.830	.614		.784
7	680	.736	6429	.840	.542		.736
7	650	.671	6038	.855	.443		.660
7	620	.576	5623	.870	.359		.623
7	603*	.530		.879		.342	.728
4	660	.808	2551	.718	.683		.845
4	630	.723	2359	.737	.551		.762
4	600	.651	2161	.757	.441		.677
4	572*	.540		.776		.358	.779
2	640	.859	1171	.549	.860		1.001
2	620	.768	1109	.568	.737		.957
2	600	.688	1046	.587	.628		.913
2	570	.571	952	.617	.488		.855
2	553*	.515		.634		.378	.779
1	570	.701	585	.415	.655		.934
1	545*	.520				.396	.825

^a Asterisk signifies sylvite saturation point. $\Gamma_{\text{H}_2\text{O}/\text{KCl}}$ signifies the ratio of activity to mole fraction of H₂O and KCl (conventional activity coefficient). $\bar{x}_{\text{H}_2\text{O}}$ is the mean H₂O mole fraction of a brucite-periclase bracket. $f_{\text{H}_2\text{O}}$ is the fugacity of H₂O at a bracket *T* and *P* (Burnham et al. 1969, with logarithmic extrapolation to 15 kbar).

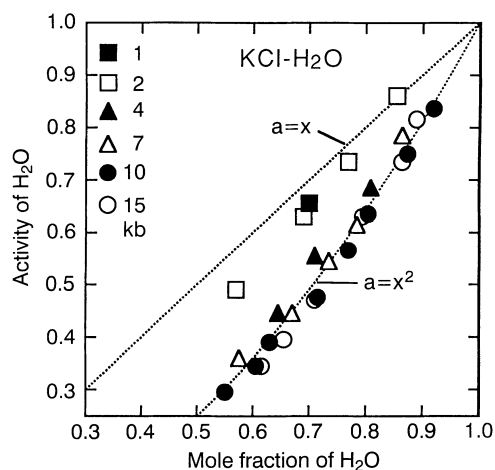


Fig. 4 H₂O activity values in concentrated KCl-H₂O solutions derived from the brucite-periclase reversal brackets of Fig. 2. Uncertainties generally somewhat smaller than symbol sizes. Note close approach of activities to the squares of the H₂O mole fractions at pressures above 4 kbar

P and *T* but not on composition of the fluid. The corresponding KCl activity coefficient is:

$$\gamma_{\text{KCl}} = \exp[W_{\text{KH}}x_{\text{H}_2\text{O}}^2] \quad (5b)$$

Least-squares analysis of the experimental data points, including the sylvite saturation points, yielded the parameters:

$$a_{\text{KCl}} = \exp(4.166 - 2.709/\rho_{\text{H}_2\text{O}}) - 212.1P/T \quad (6a)$$

$$W_{\text{KH}} = (-589.6 - 23.10P)/T \quad (6b)$$

with *P* in kbar and $\rho_{\text{H}_2\text{O}}$ in gm/cm³. Formulas based on expression 1) with these parameters reproduce all of the measured activity data to ± 0.014 .

Figure 5 shows sylvite saturation curves (or hydrous melting curves) at 0.5, 2 and 5 kbar calculated from Eqs. (1), (4)–(6). The actual DTA liquidus measurements at 0.5 and 2 kbar of Chou et al. (1992) which are directly comparable are plotted. It is seen that our equations agree perfectly with their DTA data. However, their predicted 5 kbar saturation curve lies 10 to 15 °C higher than ours at moderate H₂O contents. This discrepancy exists because their equations do not anticipate the large pressure-induced drops in H₂O and KCl activities which occur above 2 kbar.

Table 3 lists 10 kbar experiments on the brucite-periclase equilibrium with fluids in the KCl-NaCl-H₂O

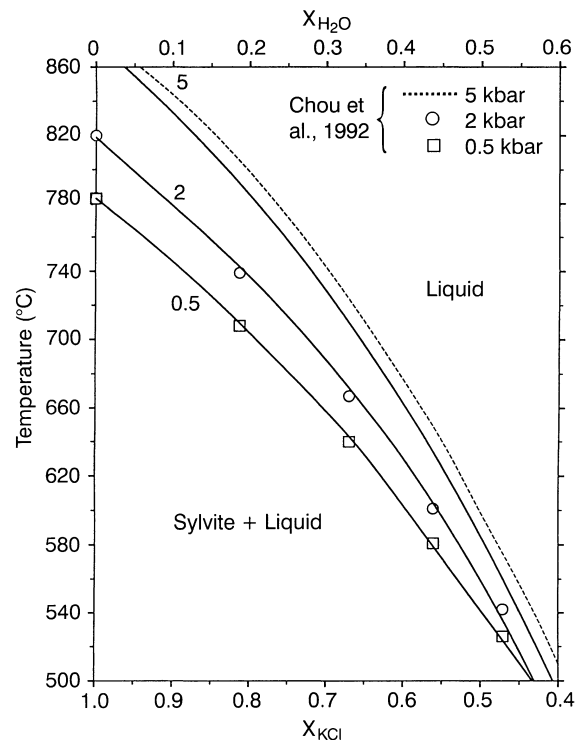


Fig. 5 Sylvite hydrous melting curves at 0.5, 2 and 5 kbar described by thermodynamic formulation of this work, Eqs. (1)–(6) (text), compared with the DTA measurements of Chou et al. (1992) at 0.5 and 2 kbar (symbols), and their predicted 5 kbar curve (dashed line). Our equations are in excellent agreement with their measurements but depart from their prediction at higher pressures because of the greater decrease of H₂O and KCl activities found in the present study

Table 3 Experimental data on the reaction $\text{Br} = \text{Per} + \text{H}_2\text{O}$ at 10 kbar in the presence of H_2O -NaCl-KCl solutions. Abbreviations as in Table 1

Run #	T °C	Duration, h	NaCl/(NaCl + KCl)	$x_{\text{H}_2\text{O}}$ st.	$x_{\text{H}_2\text{O}}$ fin.	Stable Phase
NK-14	650	139	0.492	0.53	0.568	Per
NK-15	650	139	0.518	0.613	0.575	Br
NK-12	610	119	0.501	0.461	0.5	Per
NK-13	610	119	0.516	0.533	0.507	Br
NK-3	590	240	0.504	0.3	0.38	Per, sat.
NK-4	590	240	0.364	0.3	0.36	Per, sat.
NK-10	585	142	0.352	0.282	0.23	Br, sat.
NK-11	585	142	0.491	0.294	0.26	Br, sat.

system. Experiments at 650 °C and 610 °C with NaCl/(NaCl + KCl) = 0.5 both yielded apparently reversed $x_{\text{H}_2\text{O}}$, indicating that fluids were not salt-saturated and that final vapor compositions indeed lie within the anticipated narrow T - $x_{\text{H}_2\text{O}}$ wedge of brucite-periclase-fluid stability (Fig. 6). This result shows that no marked departures exist from proportionality of $a_{\text{H}_2\text{O}}$ behavior between the two binary systems. Saturation experiments with $x_{\text{H}_2\text{O}} = 0.3$ and NaCl/(NaCl + KCl) = 0.5 and 0.35 both showed reversibility of the saturation temperature at 587 ± 3 °C. The intersection of this invariant temperature with the KCl-NaCl- H_2O saturation minimum curve, calculated as described below, gives an absolute minimum $x_{\text{H}_2\text{O}}$ of 0.45 for any fluids coexisting with

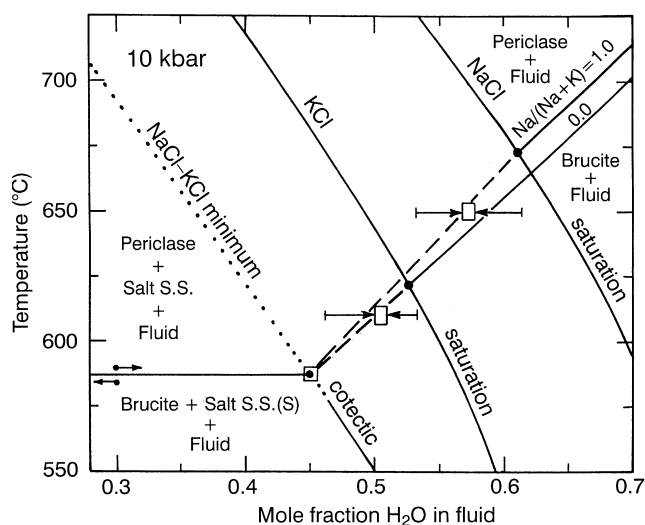


Fig. 6 Reversals of brucite-periclase equilibria in concentrated solutions of NaCl and KCl with $\text{Na}/(\text{Na} + \text{K}) = 0.5$ at 10 kbar. Data given in Table 3. Lengths of reversal arrows indicate changes of H_2O mole fraction of fluids. Ability to reverse the fluid compositions shows that vapors were not salt-saturated. Reversal arrows at $x_{\text{H}_2\text{O}} = 0.3$ bracket the temperature of brucite-periclase-crystalline salt equilibrium for $\text{Na}/(\text{Na} + \text{K})$ of 0.35 and 0.50 (no difference found). Calculations based on thermodynamic analysis indicates that the $\text{Na}/(\text{Na} + \text{K})$ of the invariant fluid is 0.38. Brucite-periclase curves for $\text{Na}/(\text{Na} + \text{K})$ of 1.0 and 0 are shown. The experimental invariant temperature of 587 ± 3 °C predicts the minimum H_2O concentration for brucite-periclase equilibrium of 0.45. Calculations indicate that the KCl-NaCl- H_2O salt saturation minimum changes from smooth minimum to cotectic at about 550 °C and $x_{\text{H}_2\text{O}} = 0.46$

periclase + brucite + Na-K chloride salts at 10 kbar. The calculations indicate that the minimum in the saturation surface is still rounded at 587 °C but becomes a cotectic at slightly lower temperatures and higher H_2O contents.

Combination of the activity expressions in the binary salt- H_2O systems into the ternary KCl-NaCl- H_2O system might be a complex problem requiring use of additional Margules parameters were it not for the close similarity of the activity behavior in the two binary systems. This similarity encourages a simple artifice: it may be assumed that the ideal activity expressions based on Eqs. (1a), (1b) may be projected proportionately into the ternary system:

$$a_{\text{KNH}}^{\text{id}} = a_{\text{KH}}^{\text{id}} \cdot \frac{x_{\text{KCl}}}{x_{\text{KCl}} + x_{\text{NaCl}}} \quad (7a)$$

$$a_{\text{NKH}}^{\text{id}} = a_{\text{NH}}^{\text{id}} \cdot \frac{x_{\text{NaCl}}}{x_{\text{KCl}} + x_{\text{NaCl}}} \quad (7b)$$

$$a_{\text{H}_2\text{O}}^{\text{id}} = a_{\text{HK}}^{\text{id}} \cdot \frac{x_{\text{KCl}}}{x_{\text{KCl}} + x_{\text{NaCl}}} + a_{\text{HN}}^{\text{id}} \cdot \frac{x_{\text{NaCl}}}{x_{\text{KCl}} + x_{\text{NaCl}}} \quad (7c)$$

Here, $a_{\text{NKH}}^{\text{id}}$ is the ideal activity of NaCl in the KNH ternary system (without the activity coefficient) and $a_{\text{NH}}^{\text{id}}$ is the same quantity in the NaCl- H_2O system based on expression (1b). The ideal ternary activities of KCl and H_2O are formulated analogously. It is seen that these expressions reduce to the appropriate binary expressions as each component individually goes to zero.

It may be shown that the formulas (7a)–(7c) satisfy the Gibbs-Duhem equation:

$$x_{\text{KCl}} d \ln(a_{\text{KNH}}^{\text{id}}) + x_{\text{NaCl}} d \ln(a_{\text{NKH}}^{\text{id}}) + x_{\text{H}_2\text{O}} d \ln(a_{\text{H}_2\text{O}}^{\text{id}}) = 0 \quad (8)$$

in general only for the special case where the dissociation parameters, α , in the KCl- H_2O and NaCl- H_2O systems are equal. This slight departure from complete generality is of no significance, however, because the α 's are so nearly equal that Eq. (7c), the expression for H_2O activity, must be valid to a high degree, though it is only an approximation to some more complex formula which satisfies the Gibbs-Duhem equation with expressions 7a and 7b.

Two modifications were made in thermodynamic formulae used in previous work, without significant loss of accuracy. The subregular solution formula of Sterner et al. (1992) for KCl-NaCl mixing in the nearly regular binary liquids was approximated as a regular solution formula by refitting their 2-kbar liquidus data. Also, the dissociation parameter in the NaCl- H_2O system of Aranovich and Newton (1996), α_{NaCl} , was recalculated in Eq. (2), along with a regular solution parameter w_{NH} , that was introduced in order to make the activity expressions for NaCl- H_2O and KCl- H_2O symmetrical. The new A, B, and C constants and the new w_{NH} parameter fitted by least squares to the measured activity data of Aranovich and Newton (1996) are given in Table 4. They reproduce the NaCl and H_2O activities in the binary system to ± 0.01 , virtually as well as in the earlier formulation. With these simplifications, the activity co-

Table 4 Parameters used in present calculations^a

Parameter	Source
$W_{KH}^F = W_{HK}^F = (-589.6 - 23.10P)/T$	This paper
$W_{NH}^F = W_{HN}^F = (109.0 - 6.89P)/T$	This paper; Aranovich and Newton (1996)
$W_{NK}^F = W_{KN}^F = -445.0/T$	Sterner et al. (1992), modified (see text)
$W_{NK}^S = (397.9 + 147.7P)/T + 9.267 - .1172P - .01773T + 8.854 \times 10^{-6}T^2$	Sterner et al. (1992) ^b
$W_{KN}^S = (970.9 + 147.7P)/T + 9.447 - .1172P - .01777T + 8.854 \times 10^{-6}T^2$	Sterner et al. (1992) ^b
$\alpha_N = \exp(4.040 - 2.902/\rho_{H_2O}) - 134.2P/T$	This paper; Aranovich and Newton (1996)
$\alpha_K = \exp(4.166 - 2.709/\rho_{H_2O}) - 212.1P/T$	This paper
$T_m(KCl) = 1043.0(P/6.9 + 1.0)^{0.1754}$	Clark (1959)
$T_m(NaCl) = 1073.5(P/16.7 + 1.0)^{0.3704}$	Clark (1959)
$\Delta V_s = -13.38 - 2.4 \times 10^{-4}(T - 298) + 0.019P$	Holland and Powell (1990)
$\Delta S_m(KCl) = 25.20$; $\Delta S_m(NaCl) = 26.22$	Robie et al. (1978)

^a *Explanations:* $\Delta G_{ij}^{xs}/RT = W_{ij}X_iX_j^2 + W_{ji}X_jX_i^2$. ΔG_{ij}^{xs} = excess Gibbs free energy of mixing in a binary join; N = NaCl; K = KCl; H = H₂O; F = fluid; S = solid; ρ_{H_2O} = density of H₂O, gm/cm³; P = pressure, kbar; T = temperature, K; α = degree of dissociation in Eqs. (1a), (1b), text; $\Delta V_s = V(\text{periclase}) - V(\text{brucite})$, cm³/mol; T_m = melting point at pressure P; ΔS_m = entropy of melting, j/K.

^b W_{NK}^S (present) = W_a^S (Sterner et al. 1992); W_{KN}^S (present) = $W_a^S + W_b^S$ (Sterner et al. 1992). The transformation is required by the slightly different Margules formulation used by Sterner et al. (1992)

efficients in the ternary system are formed from the three Margules parameters of the binary systems. The relevant equations of Sterner et al. (1992), their expressions 29 and 30, simplify to:

$$\ln \gamma_{KNH} = W_{KH}x_{H_2O}^2 + W_{KN}x_{NaCl}^2 + (W_{KN} + W_{KH} - W_{NH})x_{NaCl}x_{H_2O} \quad (9)$$

where γ_{KNH} is the activity coefficient of KCl in the ternary fluids. Symmetrical expressions exist for the activity coefficients of NaCl and H₂O.

The preceding formulation allows a simple interpretation of the α and W parameters. The ideal molecular activities of Eqs. 1a, b, expressing configurational free energy, incorporate a degree of dissociation parameter α , which should vary between zero for no dissociation of NaCl or KCl in solution to unity for complete dissociation. Additional effects of non-ideality, including solvation of solute species, devolve mainly to the W parameters of the activity coefficients. In our data fitting, the α parameters for both NaCl-H₂O and KCl-H₂O are slightly larger than one at the highest pressures, indicating that they absorb some of the non-ideality along with the W's in our simple formulation. The assumption of proportionality of binary mixing properties in the ternary system is borne out by the brucite-periclase measurements and salt saturation measurements shown in Fig. 6. As expected, the H₂O activity at a given H₂O concentration in the double salt system is intermediate between the H₂O activities in the single salt systems, and the saturation minimum curve lies at lower temperatures and lower x_{H_2O} than the saturation curve of either single salt system.

Figures 7a–d show calculated liquid-solid equilibria at 2, 5, 10 and 15 kbar for various H₂O mole fractions in the ternary system. The 2 kbar curves are nearly identical to those presented by Sterner et al. (1992). Figure 7a shows a few of the DTA liquidus data of Chou et al.

(1992) which can be compared directly with our calculated curves. Their experimental 2 kbar points fall below our calculated liquidus curves by only 4 °C at Na/(Na + K) = 0.25, 8 °C at Na/(Na + K) = 0.65, 11 °C at Na/(Na + K) = 0.45. This discrepancy parallels that between the Gunter et al. (1983) DTA liquidus data in the NaCl-H₂O system at 2 kbar and those of Aranovich and Newton (1996), which are systematically higher in temperature. The Aranovich and Newton (1996) data favor the DTA halite melting data in the NaCl-H₂O system of Koster Van Groos (1991) over those of Gunter et al. (1983). Since expressions (7) and (9) reproduce our activity data to 15 kbar very well, it is likely that calculated hydrous melting relations at pressures of 5–15 kbar are accurate. The formulas predict that the minimum melting point in the ternary system becomes very low in temperature and is shifted markedly towards KCl-rich compositions with pressure above 5 kbar. The isobaric solidus curves closely approach the solvus crest at $x_{H_2O} = 0.4$ at all pressures. At higher x_{H_2O} the salt melting minimum is of the cotectic type.

Petrologic applications

The most important feature for petrogenesis in the present work is the very low H₂O activity in concentrated alkali chloride solutions at elevated pressures. The KCl component lowers a_{H_2O} even more than does NaCl at a given T, P, and x_{H_2O} , and KCl activity is lower at a given salt concentration than NaCl activity. For this reason the isobaric ternary solidi are progressively asymmetric as pressure and x_{H_2O} increase.

The principal consequences of low H₂O activity for deep-crustal metamorphic processes are elevation of the melting temperatures of quartzofeldspathic rocks and suppression of the refractory hydrous ferromagnesian

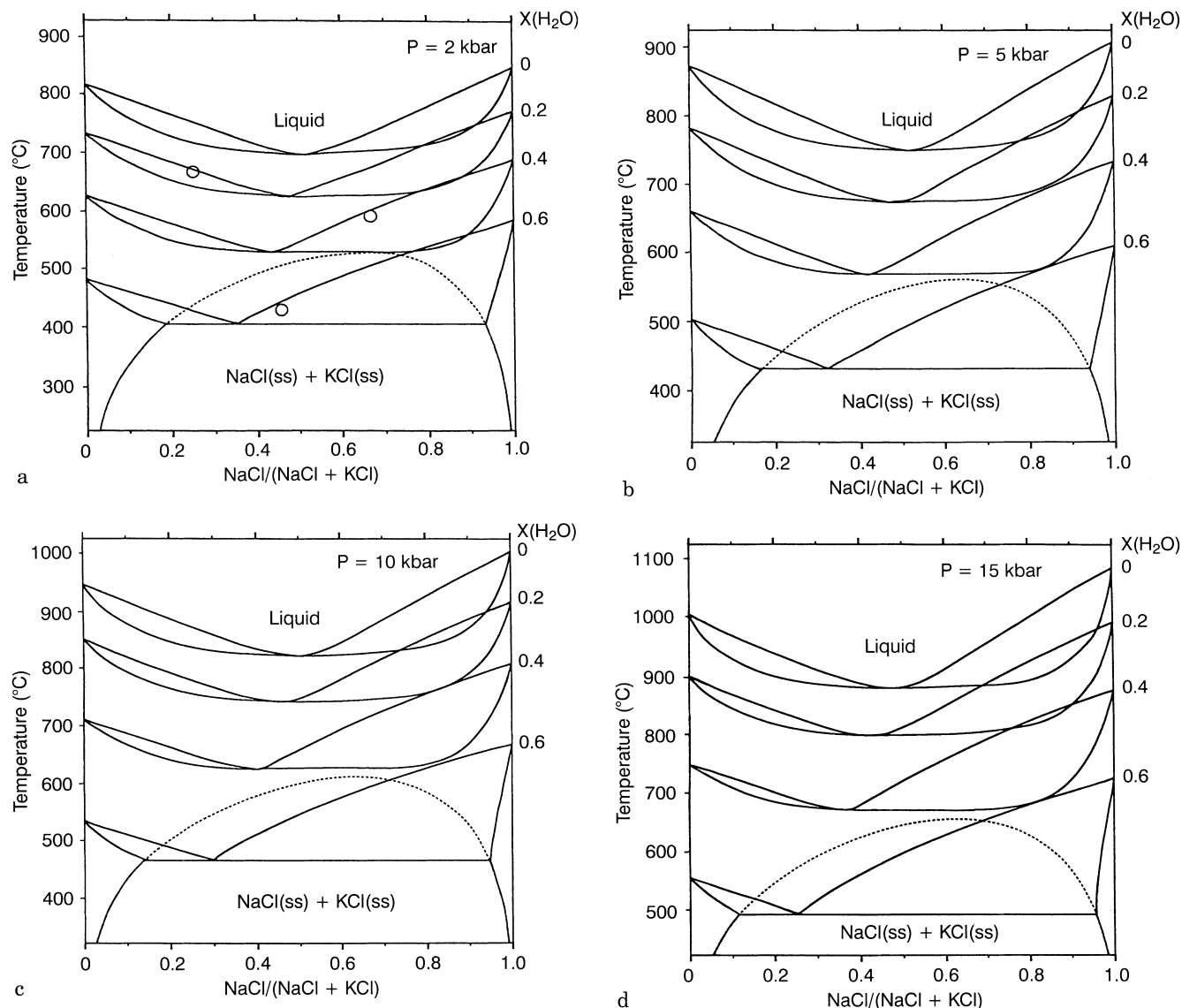


Fig. 7 Liquidus and solidus curves in the system KCl-NaCl-H₂O at 2 (a), 5 (b), 10 (c) and 15 kbar (d) described by present thermodynamic formulation. Relevant DTA measurements of Chou et al. (1992) are shown in a. The small systematic discrepancy at high H₂O mole fraction reflects a similar disagreement in the NaCl-H₂O saturation

curve between Aranovich and Newton (1996) and Gunter et al. (1983). The solvus curve (*dashed* in upper temperature interval) is from the equations of Chou et al. (1992). Alkali chloride hydrous melting is cotectic for liquids of $x_{\text{H}_2\text{O}} = 0.6$ and of the smooth minimum type at $x_{\text{H}_2\text{O}}$ less than 0.4

silicates biotite and amphibole relative to the anhydrous minerals garnet and pyroxene. Inhibition of melting allows for metamorphism and metasomatic alteration in the presence of chemically active fluids; suppression of the hydrous phases provides for stabilization of granulite facies assemblages in the presence of H₂O-bearing fluids.

The effect of concentrated alkali chloride brines on the hydrous granite solidus was calculated by Aranovich and Newton (1996). The P - T solidus curves in the system NaAlSi₃O₈(Ab)-KAlSi₃O₈(Or)-SiO₂(Qz)-H₂O-CO₂ were taken from the experimental work of Ebadi and Johannes (1991) and two simplifying assumptions were made:

(1) The granite solidus temperature is determined principally by H₂O activity. A possible effect of silicate solubility in the brine fluid was neglected. The P - T solidus points for constant $a_{\text{H}_2\text{O}}$ were taken from Ebadi and Johannes' (1991) preferred activity model.

(2) The chloride brines at the granite melting minimum are Na-dominated. This assumes that the alkali ratio near Na/(Na + K) = 0.8 of chloride solutions in equilibrium with two feldspars at elevated temperature at 1 kbar (Iiyama 1965) and 2 kbar (Orville 1963) continues to apply to higher salt concentrations and pressures.

The granite-brine P - T melting curves for constant $x_{\text{H}_2\text{O}}$ in the fluid show a remarkable effect: at pressures to

2 kbar they are nearly identical with the melting curves in the system $\text{CO}_2\text{-H}_2\text{O}$, with strongly negative dP/dT slopes at the higher H_2O mole fractions, but because of the strong decrease of $a_{\text{H}_2\text{O}}$ with increasing pressure, they bend sharply and become positive above 4 kbar. Consequently, concentrated alkali chloride solutions at higher pressures greatly elevate the hydrous granite solidus. This effect makes possible active alkali metasomatism in silicate systems at deep-crust/upper mantle conditions without large-scale melting. Concentrated brine may thus provide an intergranular medium in which alkalis are "perfectly mobile" components (Korzhinskii 1959) whose physicochemical behavior resembles that of the volatile constituents.

The present work enhances the concept of alkali mobility, with suppression of whole-rock mobility (i.e. melting). The H_2O activity is even lower at a given concentration in KCl solutions than in NaCl solutions, and is even more pressure-dependent. At deep-crustal conditions, H_2O activities in concentrated (K, Na)Cl solutions could be low enough to permit crystallization of the dense anhydrous silicates pyroxene and garnet in common quartzofeldspathic lithologies in the presence of a chemically active fluid with high infiltration capability. An important consequence of the present work is that mixture of KCl with NaCl suppresses salt saturation to lower temperatures and lower $a_{\text{H}_2\text{O}}$ than for solutions of either chloride alone, thus allowing still lower $a_{\text{H}_2\text{O}}$ in migrating fluids. Figure 8 shows the minimum $a_{\text{H}_2\text{O}}$ obtainable at 700 °C and 10 kbar, calculated from Eqs. (7) and (9) and the data of Table 4. The lowest $a_{\text{H}_2\text{O}}$ values encountered before salt saturation are less than 0.15. H_2O activities this low would permit crystallization of orthopyroxene in granulite facies assemblages in the deep crust, with suppression of biotite and amphibole (for instance, see Moecher and Essene 1991). Other

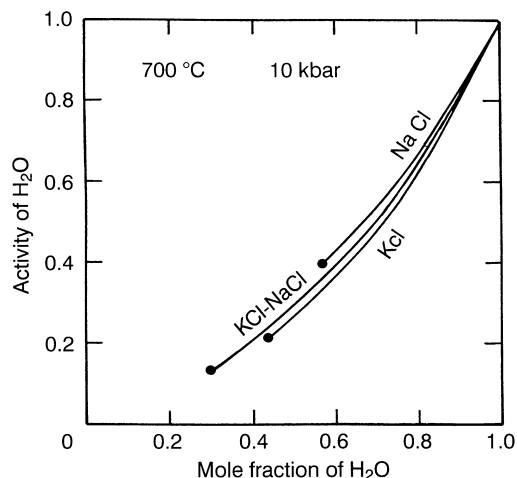


Fig. 8 H_2O activity-concentration curves at 10 kbar and 700 °C for the systems $\text{NaCl-H}_2\text{O}$, $\text{KCl-H}_2\text{O}$ and $\text{KCl-NaCl-H}_2\text{O}$ (saturation minimum). The filled circles indicate that the solutions are salt saturated. The figure shows that a mixed-salt solution can ultimately reach a H_2O activity much lower than solutions in the system $\text{NaCl-H}_2\text{O}$ before saturation occurs

ionizable solutes which would likely coexist in natural fluids, including CaCl_2 , Na_2CO_3 and $(\text{Fe, Mg})\text{SO}_4$, would further inhibit salt saturation and promote low H_2O activity.

In summary, our experimental work on H_2O activities in concentrated KCl-NaCl solutions shows that they are, in many ways, feasible as fluids of suitably low H_2O activity and high alkali mobility for a variety of deep crust and upper mantle processes. These fluids would also have the desired mechanical property of high wetting ability for silicate mineral grain boundaries, in contrast to CO_2 -rich solutions. It is likely that concentrated brines would be immiscible or only partly miscible with CO_2 under high-grade metamorphic conditions (Duan et al. 1995). A high-temperature magmatic effluent might split during ascent into CO_2 -rich and brine-rich phases, and the brines might become more concentrated by absorption of H_2O into migmatitic melts. The much greater propensity of CO_2 to be captured as fluid inclusions in silicate minerals probably has led to an exaggeration of the relative petrological role of this type of fluid (e.g. Newton 1992). Recent reports of highly saline inclusions in granulites (Touret 1996; Smit and Van Reenen 1997) indicates that this type of fluid may be a greater factor in deep-earth processes than has been assumed previously.

Acknowledgements This work was supported by a NSF grant, #EAR-9310264. Reviews by John Walther and I-Ming Chou improved the factual content and clarity of the paper. Andy Davis helped to obtain the photomicrograph of Fig. 3.

References

- Albino GV (1995) Sodium metasomatism along the Melones Fault Zone, Sierra Nevada Foothills, California, USA. *Mineral Mag* 59: 383–400
- Aranovich LYa, Newton RC (1996) H_2O activity in concentrated NaCl solutions at high pressures and temperatures measured by the brucite-periclase equilibrium. *Contrib Mineral Petrol* 125: 200–212
- Aranovich LYa, Shmulovich KI, Fedkin VV (1987) The H_2O and CO_2 regime in regional metamorphism. *Int Geol Rev* 29: 1379–1401
- Bhardwaj MC, Roy R (1971) Effect of high pressure on crystalline solubility in the system NaCl-KCl . *Phys Chem Solids* 32: 1603–1607
- Billings MP (1938) Introduction of potash during regional metamorphism in western New Hampshire. *Geol Soc Am Bull* 49: 289–302
- Burnham CW, Holloway JR, Davis NF (1969) Thermodynamic properties of water to 1,000 °C and 10,000 bars. *Geol Soc Am Spec Pap* 132
- Chou I-M, Sterner SM, Pitzer KS (1992) Phase relations in the system $\text{NaCl-KCl-H}_2\text{O}$: IV. Differential thermal analysis of the sylvite liquidus in the $\text{KCl-H}_2\text{O}$ binary, the liquidus in the $\text{NaCl-KCl-H}_2\text{O}$ ternary, and the solidus in the NaCl-KCl binary to 2 kb pressure, and a summary of experimental data for thermodynamic-PTX analysis of solid-liquid equilibria at elevated P-T conditions. *Geochim Cosmochim Acta* 56: 2281–2293
- Clark SP Jr (1959) Effect of pressure on the melting point of eight alkali halides. *J Chem Phys* 31: 1526–1531
- DeJong G, Williams PJ (1995) Giant metasomatic system formed during exhumation of mid-crustal Proterozoic rocks in the vicinity of the Cloncurry Fault, northern Queensland. *Aust J Earth Sci* 42: 281–290

- Duan Z, Møller N, Weare JH (1995) Equation of state for the NaCl-H₂O-CO₂ system: prediction of phase equilibria and volumetric properties. *Geochim Cosmochim Acta* 59: 2869–2882
- Dunbar NW, Campbell AR, Candela PA (1996) Physical, chemical, and mineralogical evidence for magmatic fluid migration within the Capitan pluton, southeastern New Mexico. *Geol Soc Am Bull* 108: 318–333
- Ebadi A, Johannes W (1991) Beginning of melting and composition of first melts in the system Qz-Ab-Or-H₂O-CO₂. *Contrib Mineral Petrol* 106: 286–295
- Griffin WL (1969) Replacement antiperthite in gneisses of the Babbitt-Embarrass area, Minnesota, USA. *Lithos* 2: 171–186
- Gunter WD, Chou I-M, Girsperger S (1983) Phase relations in the system NaCl-KCl-H₂O: differential thermal analysis of the halite liquidus in NaCl-H₂O binary above 450 °C. *Geochim Cosmochim Acta* 47: 863–873
- Hansen EC, Newton RC, Janardhan AS, Lindenberg S (1995) Differentiation of Late Archean crust in the Eastern Dharwar Craton, South India. *J Geol* 103: 629–651
- Holland TJB, Powell R (1990) An enlarged and updated internally consistent thermodynamic dataset with uncertainties and correlations: the system K₂O-Na₂O-CaO-MgO-MnO-FeO-Fe₂O₃-Al₂O₃-TiO₂-SiO₂-C-H₂O₂. *J Metamorphic Geol* 8: 89–124
- Iiyama JT (1965) Influence des anions sur les équilibres d'échange d'ions Na-K dans les feldspaths alcalins à 600 °C sous une pression de 1000 bars. *Bull Soc Fr Minéral Cristalogr* 88: 618–622
- Korzhinskii DS (1959) Physicochemical basis of the analysis of the paragenesis of Minerals. Consultants Bureau, New York
- Koster Van Groos AF (1991) Differential thermal analysis of the liquidus relations in the system NaCl-H₂O to 6 kbar. *Geochim Cosmochim Acta* 55: 2811–2817
- Moecher DP, Essene EJ (1991) Calculation of CO₂ activity using scapolite equilibria: constraints on the presence and composition of a fluid phase during high grade metamorphism. *Contrib Mineral Petrol* 108: 219–240
- Newton RC (1992) Charnockitic alteration: evidence for CO₂ infiltration in granulite facies metamorphism. *J Metamorphic Geol* 10: 383–400
- Orville PM (1963) Alkali ion exchange between vapor and feldspar phases. *Am J Sci* 261: 201–237
- Pasteris JD, Harris TN, Sassari DC (1995) Interactions of mixed volatile-brine fluids in rocks of the southwestern footwall of the Duluth Complex, Minnesota – evidence from aqueous fluid inclusions. *Am J Sci* 295: 125–172
- Philippot P, Selverstone J (1991) Trace-element-rich brines in eclogitic veins: implications for fluid composition and transport during subduction. *Contrib Mineral Petrol* 106: 417–430
- Philippot P, Chevallier P, Chopin C, Dubessy J (1995) Fluid composition and evolution in coesite-bearing rocks (Dora Maira massif, western Alps): implications for element recycling during subduction. *Contrib Mineral Petrol* 121: 29–41
- Quist AS, Marshall WL (1969). The electrical conductances of some alkali metal halides in aqueous solutions from 0–800 °C and at pressure to 4000 bars. *J Phys Chem* 73: 978–985
- Quist AS, Marshall WL, Franck EU, von Osten W (1970). A reference solution for electrical conductance measurements to 800 °C and 12,000 bars. Aqueous 0.01 molal potassium chloride. *J Phys Chem* 74: 2241–2243
- Robie RA, Hemingway BS, Fisher JR (1978) Thermodynamic properties of minerals and related substances at 298.15 K and 1 bar (10⁵ pascals) pressure and at higher temperatures. *US Geol Surv Bull* 1452: 1–456
- Sampson IM, Liu W, Williams-Jones AE (1995) The nature of orthomagmatic fluids in the Oka carbonatite, Quebec, Canada: evidence from fluid inclusions. *Geochim Cosmochim Acta* 59: 1963–1977
- Smit CA, Van Reenen DD (1997) Deep crustal shear zones, high grade tectonites, and associated metasomatic alteration in the Limpopo Belt, South Africa: implications for deep-crustal processes. *J Geol* 105: 37–58.
- Sterner SM, Chou I-M, Downs RT, Pitzer KS (1992) Phase relations in the system NaCl-KCl-H₂O: V. Thermodynamic-PTX analysis of solid-liquid equilibria at high temperatures and pressures. *Geochim Cosmochim Acta* 56: 2295–2309
- Todd CS, Evans BW (1994) Properties of CO₂-induced dehydration of amphibolite. *J Petrol* 35: 1213–1240
- Touret JLR (1985) Fluid regime in southern Norway: the record of fluid inclusions. In: Tobi AC, Touret JLR (eds) *The deep Proterozoic crust in the North Atlantic provinces*. Reidel, Dordrecht pp 517–549
- Touret JLR (1996) Fluids in granulites: the quest continues. *V.M. Goldschmidt Conference Heidelberg, Germany*, 1: 623
- Walther JV (1992) Ionic association in H₂O-CO₂ fluids at mid-crustal conditions. *J Metamorphic Geol* 10: 789–797
- Watson ED, Brenan JM (1987) Fluids in the lithosphere, 1. Experimentally-determined wetting characteristics of CO₂-H₂O fluids and their implications for fluid transport, host-rock physical properties, and fluid inclusion formation. *Earth Planet Sci Lett* 85: 497–515